Microcalorimetric Quantification of Hydrogen Adsorption Thermodynamics in Water-Solvated Systems on Pt/C

Supplementary Information

William T. Broomhead and David W. Flaherty*

School of Chemical and Biomolecular Engineering, Georgia Institute of Technology, Atlanta, GA 30032, United States

* Corresponding author. dflaherty3@gatech.edu

S1. N_2 Physisorption Isotherms of Pt Catalysts

Figure S1 provides the N_2 adsorption-desorption isotherms for Pt/C and Pt/Al_2O_3 catalysts at 77 K. Specific surface areas were estimated from uptakes in N_2 activity (P/P^0) range of 0.05–0.3 following the method of Brunauer, Emmett, and Teller (BET). For Pt/C, this method gives specific surface areas of 106 ± 8 $m^2\ g^{-1}$.

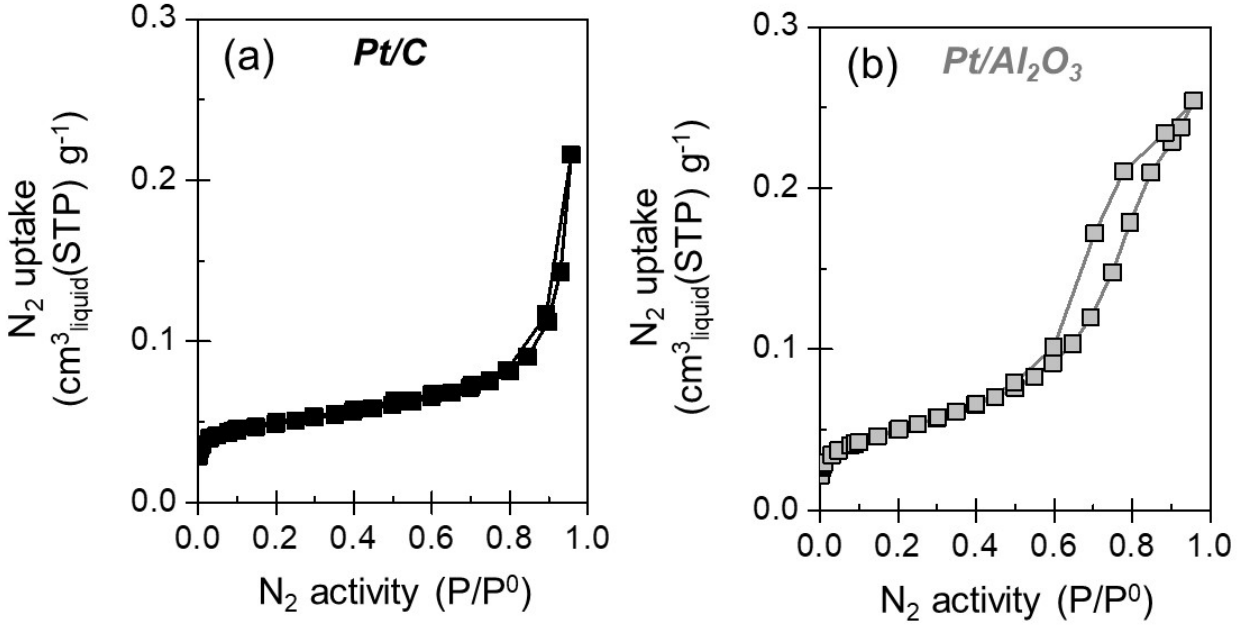

Figure S1. N_2 physisorption isotherms for (a) Pt/C and (b) Pt/Al_2O_3 catalysts. Solid lines are provided to guide the eye.

S2. Transmission Electron Microscopy of Pristine Pt/C Catalysts

Figure S2 provides a representative transmission electron micrograph of the Pt/C catalysts.

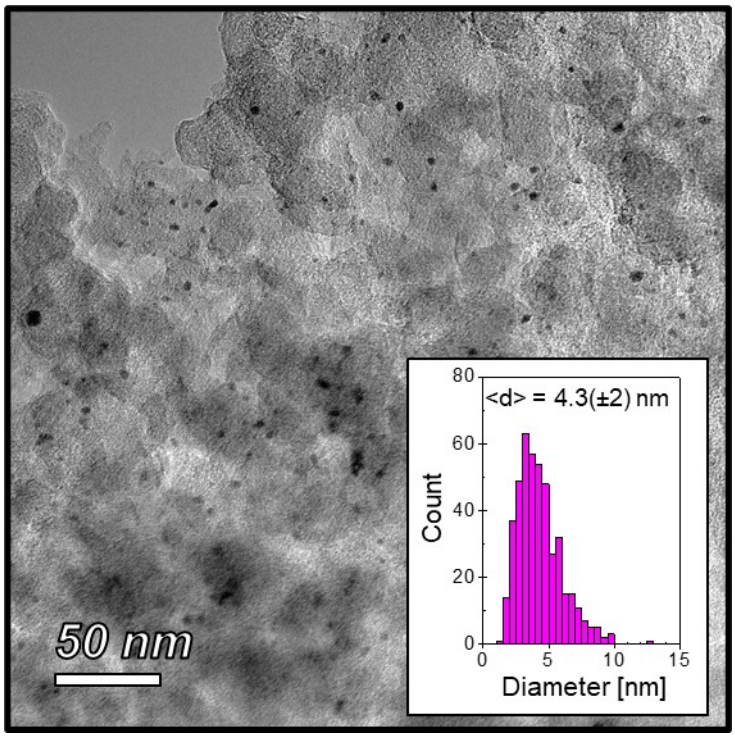

Figure S2. Transmission electron micrograph of Pt/C catalysts with a histogram of cluster diameters provided as an inset.

S3. Schematic and Operation of the Isothermal Adsorption Calorimetry System

Figure S3 provides a schematic representation of the system used for isothermal adsorption calorimetry in this study. The system connects a volumetric adsorption device (Micromeritics, 3Flex) with precise control over the molar quantities of delivery gases as well as H_2O vapor, connected to a vacuum ampoule for insertion in an isothermal microcalorimeter (TA instruments, TAM IV). A flexible stainless steel tubing connection between the two instruments enabled movement between a treatment zone—where catalysts were exposed to temperatures up to 473 K—and the calorimeter while retaining a dynamic evacuation. We emphasize that both systems are commercially available and flexible for a wide range of adsorbents, adsorbates, and solvent environments.

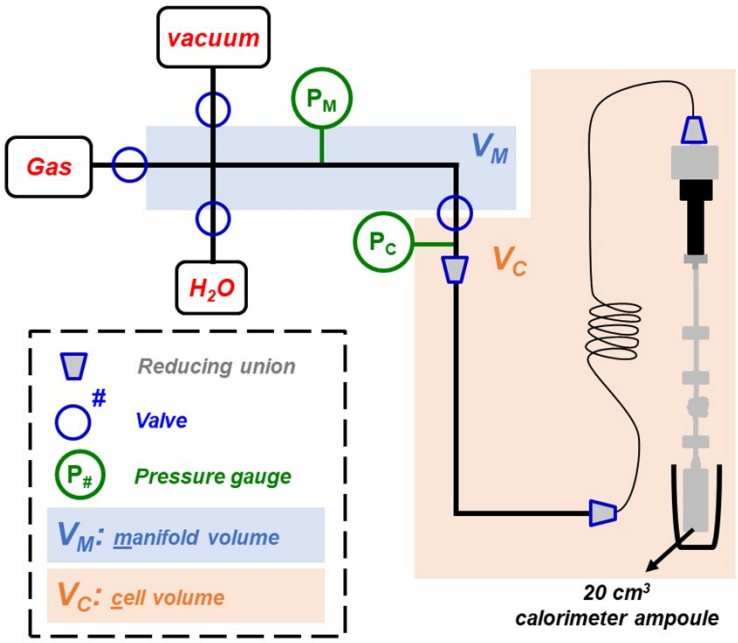

Figure S3. Simplified schematic of a connected volumetric adsorption-microcalorimeter system.

For each dose, the volumetric adsorption device enabled precise quantification of both the number of moles dosed (n_{dose}) and pressure change (ΔP) while the calorimeter provided the cumulative heat flow ($Q_{measured}$). The molar uptake (Δn_{ads}) equals the difference in n_{dose} and the final number of moles (n_{final}) accounting for the number of moles initially in the system prior to each dose ($n_{initial}$):

$$\Delta n_{ads} = n_{dose} - (n_{final} - n_{initial}) \quad \text{(S3.1)}$$

Eqn. S3.1 applies for each component. Doses of He, CO, and H_2 gases in the presence of H_2O but in non-adsorbing environments (i.e., $^{\Delta n_{ads}} = 0$, Figure S4a) calibrate the gas expansion through $^{\Delta P}$ to give $^{n_{final}}$ following the ideal gas law (pressure, temperature, and volume subscripts referring to manifold and cell in Figure S3):

$$n_{dose} = n_{final} - n_{initial} = \frac{1}{R}\left(\frac{V_m}{T_m} + \frac{V_c}{T_c}\right)\Delta P_c \tag{S3.2}$$

In each dose, measured heat flows ($^{Q_{measured}}$) consisted of contributions from adsorption ($^{Q_{ads}}$) as well as gas expansion $^{Q_{expansion}}$, the latter due to the increase in the number of molecules of gas in the calorimeter control volume:

$$Q_{measured} = Q_{ads} + Q_{expansion} \tag{S3.3}$$

Expansion heats tended to follow power law relations with respect to $^{\Delta P}$ but differed for each adsorbate mixture due to differences in the heat capacities of each gas composition. Thus, $^{Q_{expansion}}$ values were estimated at the end of each adsorption experiment when $^{\Delta n_{ads}}$ approached zero; validating this approach with He reveals a negligible enthalpy of He adsorption ($^{\Delta H_{ads,He}} = - Q_{ads}$, Figure S4b).

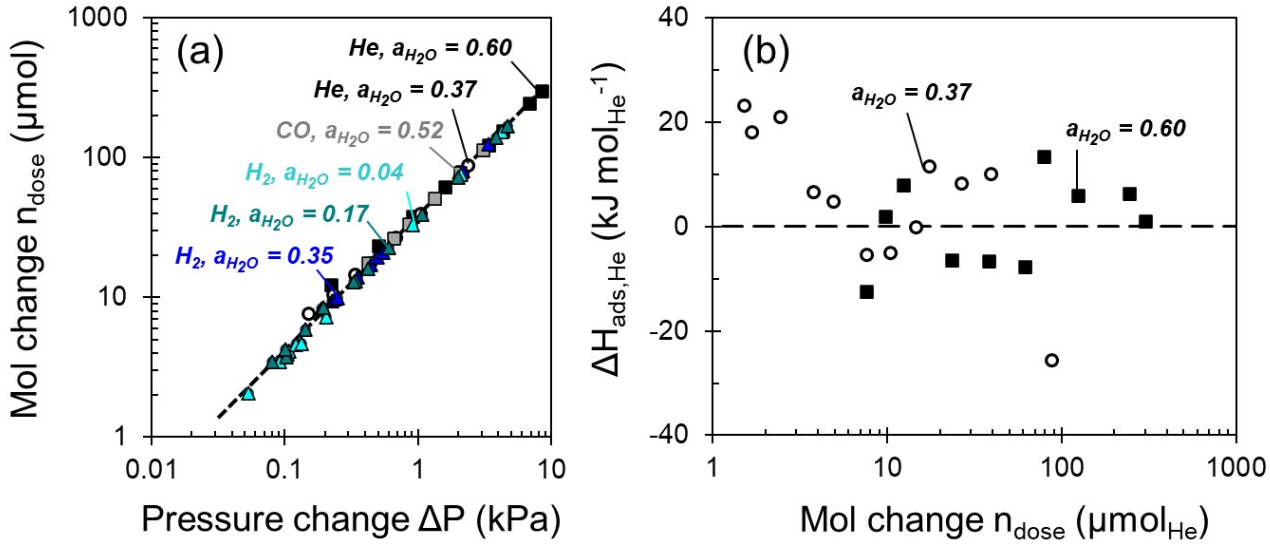

Figure S4. Validation of (a) cell volume calculations (Eqn. S3.2) for He (black), CO (gray), and H_2 (blue) and (b) expansion heat calibration methods for He ($^{\Delta H_{ads,He}} = - Q_{ads} = 0$). 1.0 g Pt/C, 298 K.

Prior to adsorption measurements with H_2O, a molar quantity of H_2O vapor was introduced to reach its desired thermodynamic activity. Figure S5 provides the H_2O adsorption isotherm for Pt/C as the molar uptake (primary y-axis) and the average H_2O per nm^2 (secondary y-axis).

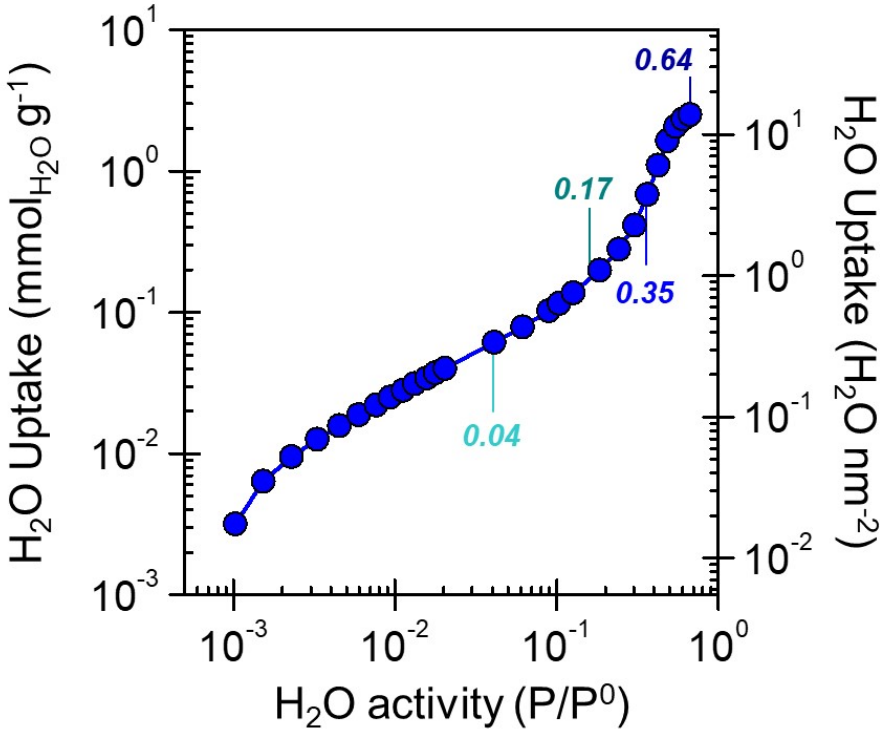

Figure S5. H_2O adsorption isotherm on Pt/C at 298 K. Saturation pressure P^0 equals 3.1 kPa. Solid line provided to guide the eye.

S4. Adsorption Isotherms for CO and H_2 in the Absence of Water

Figure S6 provides the adsorption isotherms for H_2 and CO on Pt/C in the absence of H_2O. Normalizing the molar uptakes by the Pt site density (11 μmol-Pt_{surf} g^{-1}) gives the fractional coverages of adsorbates (x-axis of Figure 1a of the main text). For reference, adsorption isotherms and differential heats of CO adsorption on Pt/Al_2O_3 standards are provided (Figure S7).

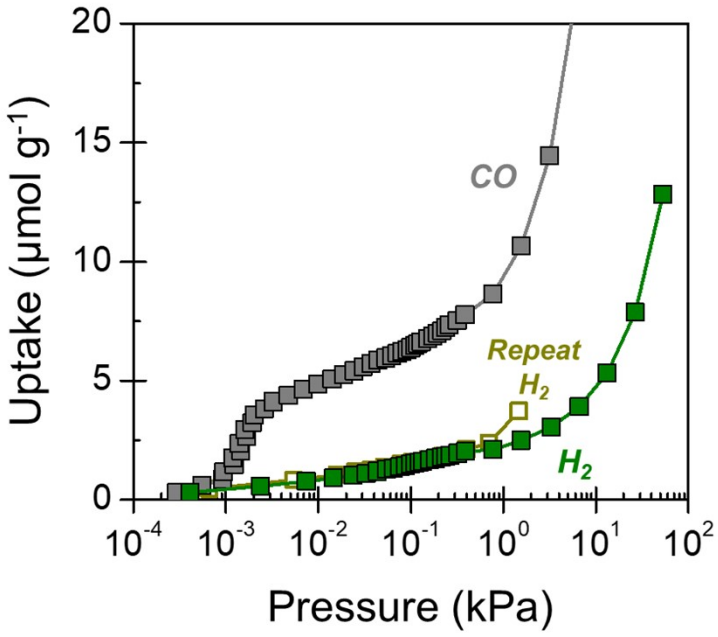

Figure S6. H_2 (green and gold) and CO (gray) adsorption isotherms in the absence of H_2O (4.3 nm Pt/C, 298 K). Solid lines are provided to guide the eye.

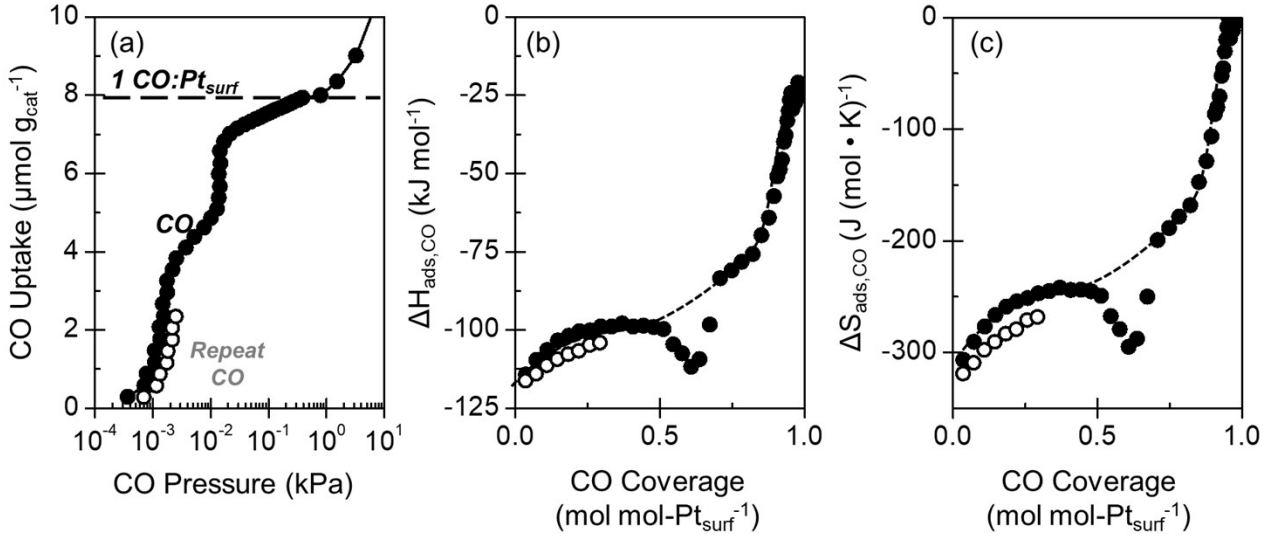

Figure S7. Adsorption isotherms (a), enthalpies ($\Delta H_{ads,CO}$, b), and entropies ($\Delta S_{ads,CO}$, c) for CO uptakes on Pt/Al_2O_3 reference materials as a function of coverage in the absence of H_2O (298 K). Dashed lines are provided to guide the eye.

S5. Adsorption Isotherms for H_2 on Pt/C with Varying Water Activities

Figure S8 provides the H_2 adsorption isotherms on Pt/C at varying activities of water (a_{H_2O}). Upon adding water, hydrogen uptakes vastly exceed their anhydrous counterparts, with a maximum uptake approaching 100 μmol-H_2 g^{-1} (20 mol-H (mol-Pt_{surf})$^{-1}$). Normalizing the H_2 uptakes (Figure S8a) by the volumetric uptake of water (Figure S5) collapses the distinct adsorption isotherms to a single profile (Figure S8b). Instantaneous adsorption free energies $\Delta G_{ads,H}$ at each distinct H_2 coverage were evaluated from this relation following Eqn. 4 of the main text.

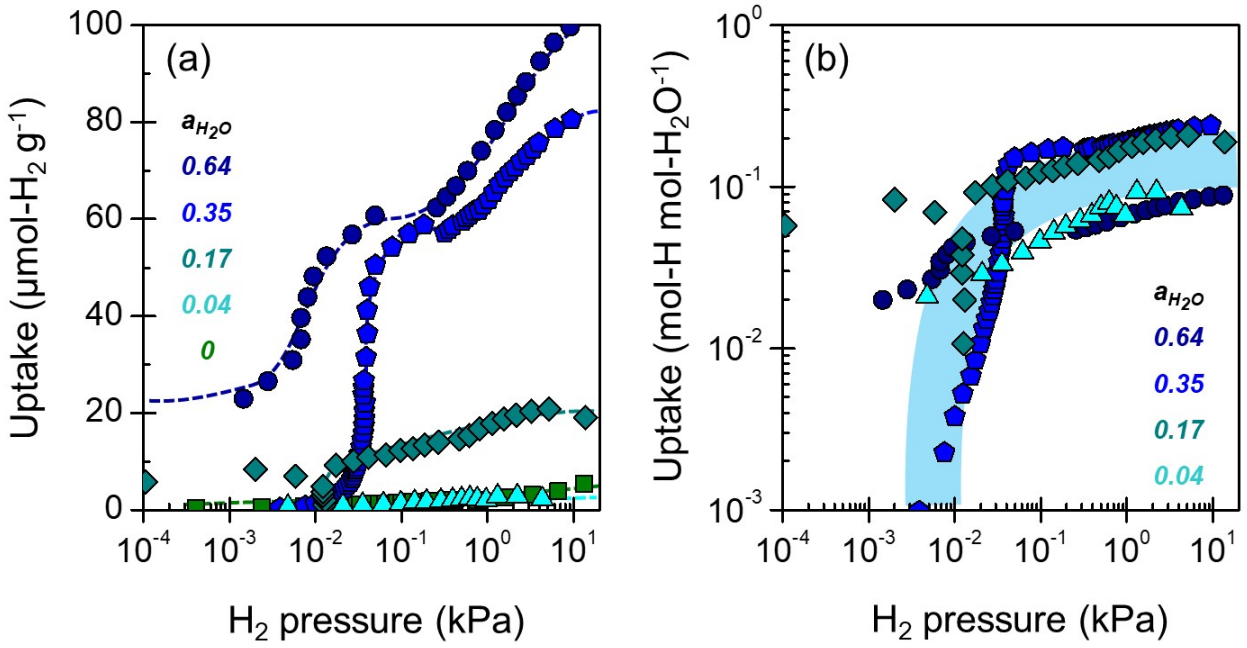

Figure S8. (a) Hydrogen adsorption isotherms with varying thermodynamic activities of H_2O. (b) Hydrogen uptakes normalized by the quantity of adsorbed water (mol-H mol-H_2O^{-1}) versus H_2 pressure. 4.3 nm Pt/C, 298 K. Dashed and shaded lines are provided to guide the eye.

S6. Effects of Intraparticle Carbon Dilution on Uptakes and Heats of H_2 Adsorption on Pt/C

Figure S9 provides the adsorption isotherms and differential heats of hydrogen adsorption on Pt/C with a 1-to-6.3 Pt/C-to-C (mass basis) intraparticle dilution, and either in the presence or absence of H_2O. Under anhydrous conditions, adsorption isotherms are slightly offset to higher uptakes in the diluted sample. Hydrogen adsorption enthalpies approach zero before 1.0 mol-H (mol-Pt_{surf})$^{-1}$, confirming that the offset in adsorption isotherms is not due to uptake on the bare C diluent. Exposing each catalyst to H_2O at an activity of 0.35 ± 0.02 gives the same H_2O uptake normalized by the total sample mass (approximately 0.7 mmol-H_2O g^{-1}, Figure S5). Hydrogen uptakes for these two samples reach comparable values when normalized by the number of Pt sites but a large offset when normalized by the number of H_2O molecules. In the absence of electrical connectivity between Pt/C particles and C diluents, this diluent effect agrees with the capacitive interaction mechanism of Scheme 2.

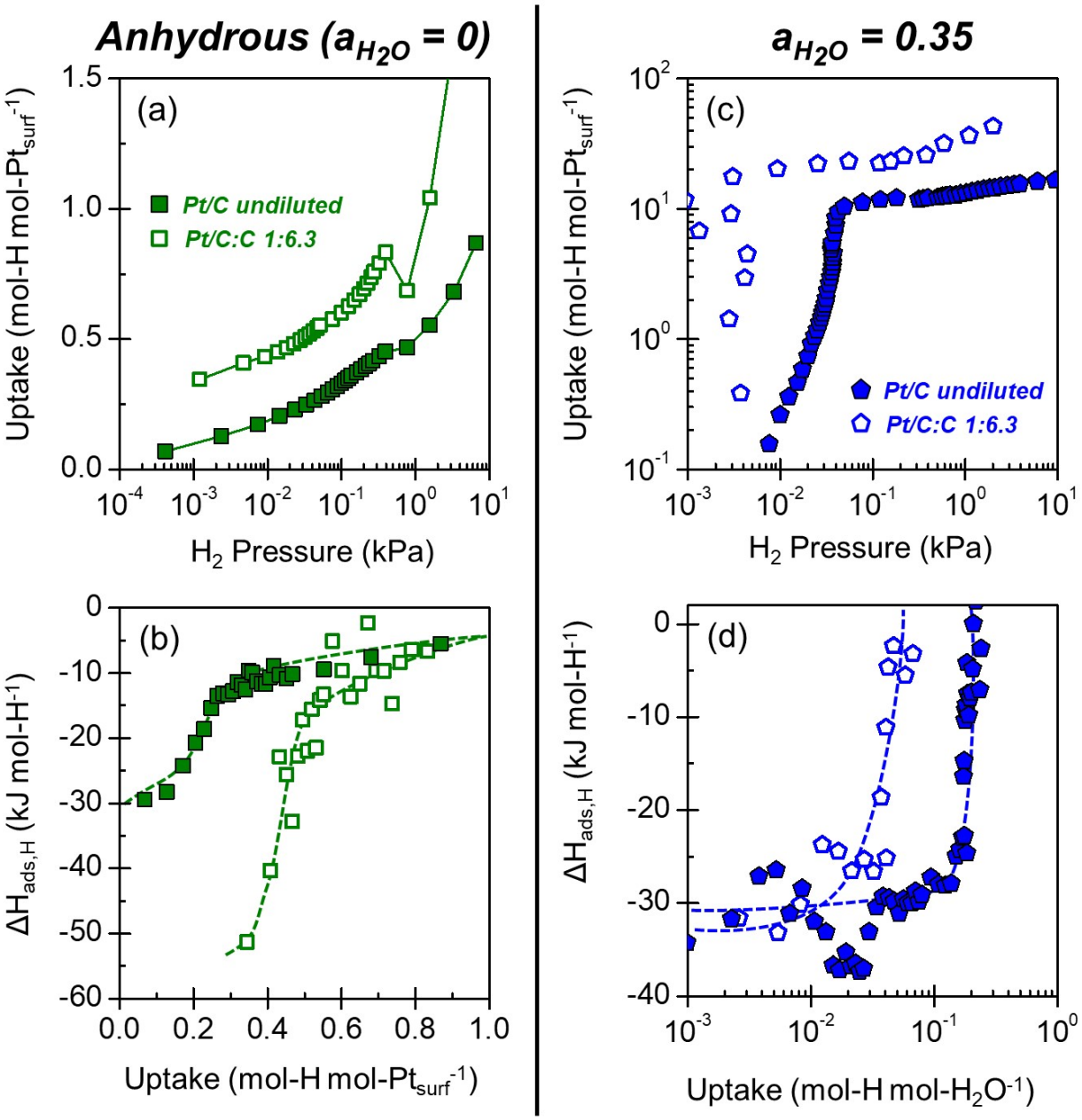

Figure S9. Effects of a 7-fold intraparticle dilution of Pt/C with C (undiluted: solid points, diluted: hollow points) under (a–b) anhydrous and (c–d) H_2O containing conditions (H_2O activity of 0.35) on (a or c) hydrogen uptakes normalized per Pt surface sites and (b or d) adsorption enthalpies as a function of H uptakes per Pt (b) or per H_2O (d). 1.0 g total 4.3 nm Pt/C or Pt/C + C, 298 K.

S7. Differential Enthalpies, Entropies, and Free Energies for Hydrogen Adsorption on Pt/C

Figure S10 provides the hydrogen adsorption enthalpies ($\Delta H_{ads,H}$), entropies ($\Delta S_{ads,H}$), and free energies ($\Delta G_{ads,H}$) evaluated at varying hydrogen coverages and water activities. Instantaneous $\Delta G_{ads,H}$ values vary minimally among all conditions.

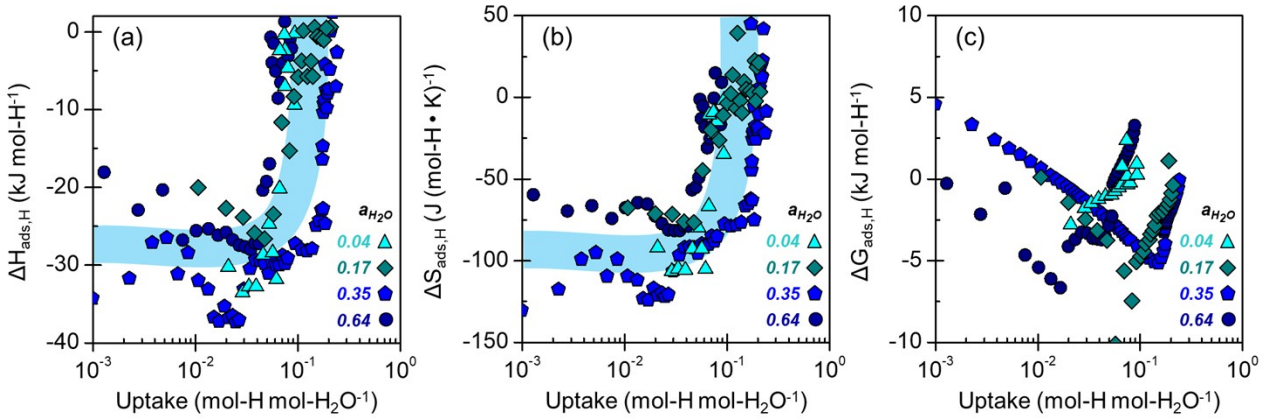

Figure S10. Hydrogen adsorption enthalpies (a, $\Delta H_{ads,H}$), entropies (b, $\Delta S_{ads,H}$), and free energies (c, $\Delta G_{ads,H}$) as a function of hydrogen coverage normalized by the quantity of adsorbed water. 4.3 nm Pt/C, 298 K. Shaded lines are provided to guide the eye.

S8. Gas Phase Batch Profiles and CO Consumption Rates on Pt/C

Figure S11 provides the batch CO consumption profiles and derived CO consumption rates ($-r_{CO}$) on Pt/C with varying H_2O activity. The emergence of new H_2O-assisted activation pathways leads to $-r_{CO}$ values which increase by nearly an order of magnitude upon H_2O introduction, analogous to the findings for H_2 adsorption (Figure 2 of the main text).

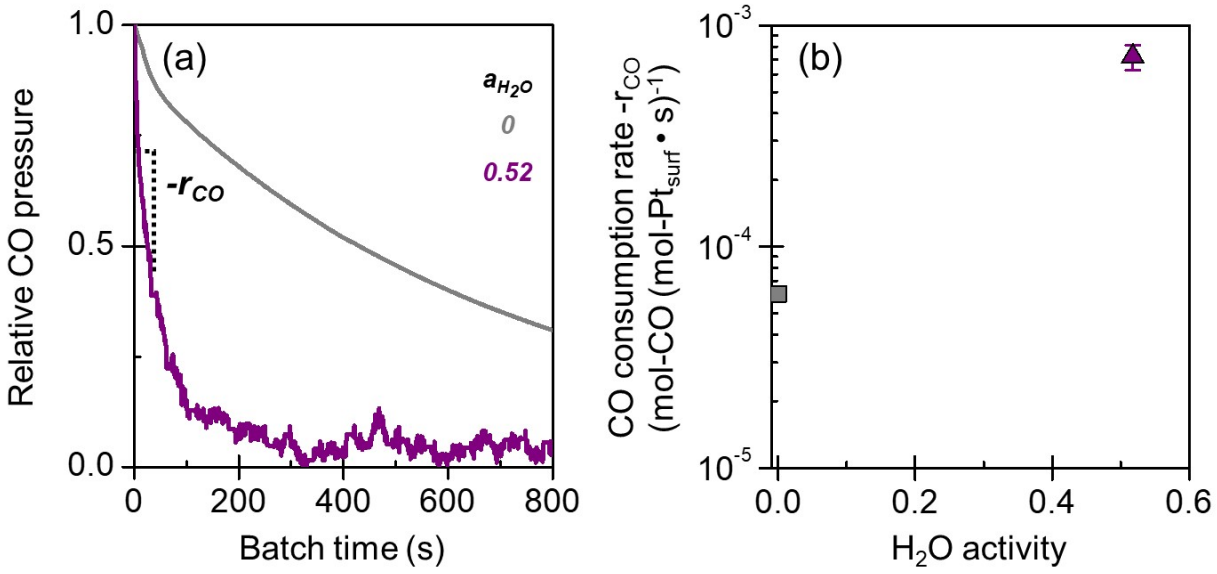

Figure S11. (a) Gas phase batch profiles for CO molar consumption and (b) initial rates of CO consumption with varying thermodynamic activities of H_2O. 4.3 nm Pt/C, 298 K. Error margins reflect 95% confidence intervals of five CO doses.

S9. Adsorption Isotherms and Differential Heats for CO Adsorption on Pt/C with Water

Figure S12 provides the isotherms, enthalpies ($\Delta H_{ads,CO}$), and entropies ($\Delta S_{ads,CO}$) for CO adsorption in the presence of water ($a_{H_2O} = 0.52$) on Pt/C. $\Delta S_{ads,CO}$ values were estimated from a capacitive adsorption model analogous to Scheme 2 of the main text, treating H_2O as the active site. Saturation CO uptakes (defined when $\Delta H_{ads,CO}$ reaches 0 kJ mol^{-1}) exceed the monolayer coverage of Pt, equaling 5 mol-CO (mol-Pt$_{surf}$)$^{-1}$, likely due to CO spillover onto the carbon support facilitated by H_2O. Upon introducing H_2O, adsorption enthalpies extrapolated to zero coverage weaken by introducing water ($\Delta H_{ads,CO}$ increasing from -91 ± 4 kJ mol^{-1} to -50 ± 10 kJ mol^{-1}), likely due to dipole and van der Waal's interactions between CO and H_2O that weaken the Pt-C bonds in CO adsorbed states.

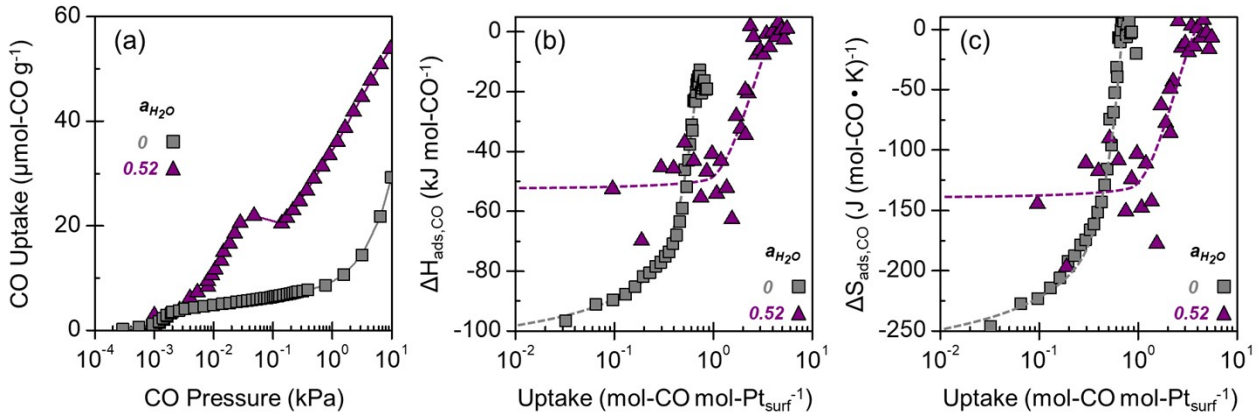

Figure S12. Effects of H_2O on (a) CO molar uptakes as a function of pressure, (b) CO adsorption enthalpies, and (c) CO adsorption entropies as a function of CO coverage. 4.3 nm Pt/C, 298 K. Dashed and solid lines are provided to guide the eye.